Perpendicular-space fluctuations and diffraction-peak-intensity scaling of two-dimensional twins and quasi-crystals

1991 J. Phys.: Condens. Matter 3 2457

(http://iopscience.iop.org/0953-8984/3/15/001)

J. Phys.: Condens. Matter 3 (1991) 2457–2470. Printed in the UK

Perpendicular-space fluctuations and diffraction-peak-intensity scaling of two-dimensional twins and quasi-crystals

Janusz Wolny and Lucjan Pytlik
Institute of Physics and Nuclear Techniques, Academy of Mining and Metallurgy, al. Mickiewicza 30, 30-059 Kraków, Poland

Received 28 June 1990, in final form 2 January 1991

Abstract. Various two-dimensional structures, i.e. Penrose tiling, twins, and random and precipitated structures, obtained by tiling the plane using Robinson triangles and decoration with two types of sites have been analysed in five-dimensional hyperspace. Diffraction peak intensities for all these structures can be well approximated by the Debye–Waller factor calculated in perpendicular (phason) space. Mean-square values of perpendicular-space fluctuations scale linearly with the number of sites for all concentrations of small Robinson triangles except the Penrose concentration. The slope coefficient exhibits critical behaviour at the Penrose concentration, with critical exponent equal to 1. The derived value of the critical exponent for the scaling factor, describing the scaling of the peak intensities, is equal to 0.5. At the Penrose concentration the linear term in the mean-square perpendicular space fluctuation dependence on the number of sites vanishes and, for random Penrose tiling, a logarithmic term becomes dominant, significantly changing the dependence of peak intensities on the number of sites. For all the structures discussed above, analytical expressions for peak intensities have been tested.

1. Introduction

There are many theoretical concepts explaining diffraction patterns exhibiting forbidden symmetry like those discovered by Shechtman (Shechtman *et al* 1984). The first such concept had been known even before that famous discovery and was given by Penrose (1974), who discovered non-periodic tilings of the plane using only two non-equivalent elements. Later de Bruijn (1981) extended this concept and also showed that the construction could be interpreted as the projection of a five-dimensional lattice structure onto a two-dimensional subspace. The projection method was used by Kramer and Neri (1984) to construct a three-dimensional generalization of the Penrose tiling by projection from six dimensions. Another concept is a crystal twinning proposed by Field and Fraser (1984) and Pauling (1985, 1987). Recently the random quasi-crystalline structures obtained by the growth method, i.e. by attaching tiles to an existing seed (Stephens and Goldman 1986, Minchau *et al* 1987, Nori *et al* 1988, Wolny *et al* 1988, 1990, Lebech *et al* 1988, Onoda *et al* 1988, Tang and Jarić 1990), or in the thermodynamically equilibrated version by the Monte Carlo method (Widom *et al* 1987, Strandburg *et al* 1989), and

0953-8984/91/152457 + 14 $03.50

molecular dynamics (Lançon and Billard 1988) have been extensively studied. New tilings of the plane using Robinson triangles have been discussed by Godreche and Luck (1989). Theoretical explanations for such structures using transfer matrix calculations (Henley 1988, Widom *et al* 1989) have also been presented. Calculations of the diffraction patterns using the projection method can also be found (Jarić 1986, Elser 1985, 1986, Henley 1988).

This paper continues the discussion of similarities of various structures obtained by tiling the plane using only two types of Robinson triangles, and presented in our previous papers (Wolny *et al* 1988, 1990, further called I and II). Penrose and random Penrose structures can be obtained by the inflation method (I and II and references therein), where each large triangle gives two large triangles and a small one, and each small triangle gives one large and one small triangle. Random and precipitated structures have been obtained by random attachment of Robinson triangles to the existing seed under the strict condition that the plane should be filled without defects. The random structures exhibit short-range correlations and are subject to the condition that the concentration of the small Robinson triangles is restricted to a very narrow region near the Penrose tiling value ($c_P = 1/\tau^2 \simeq 0.382$, I). If the concentration differs much from the Penrose concentration, coherent precipitations of microcrystals emerge in the structure.

Correlation functions and diffraction patterns of all those structures have 10-fold (or nearly 10-fold) symmetry and the diffraction patterns consist of well defined peaks. Additionally, the diffraction patterns exhibit the same series of peaks as those observed for Penrose tiling; however, only for this particular tiling peak do maxima scale with N^2 as in classical crystallography. For twin and precipitated structures, groups of peaks are observed instead of single peaks. The peaks in one group overlap for high values of the scattering vector, giving maxima at the Penrose positions. For twins, however, in all groups single peaks can be resolved if a large enough number of sites is included in the cluster, which is never observed for random structures. Using the Penrose structure as a reference structure, a universal function describing the dependence of peak intensities against $\ln(k)$ (where k is the scattering vector) has been found, and a linear relation between the scaling factor (defined in II) and the size of the cluster has been obtained. The slope coefficient of this linear relation exhibits a singular dependence on the concentration of small Robinson triangles, having a singular point at the Penrose concentration. The critical exponent for this dependence was found to be equal to 0.55 ± 0.02.

In this paper we are using the concept of perpendicular- or phason-space fluctuations having an influence on peak intensities calculated at Penrose positions of scattering vectors (Jarić 1986, Henley 1988, Tang and Jarić 1990). We calculated these fluctuations for all discussed structures described by different concentration or way of tiling the plane (ordered or random). Using a Debye–Waller approximation for phason-space fluctuations, we have explained the similarities of the diffraction patterns for those structures observed in I and II.

2. Definition of structures

As mentioned before, the structures discussed in this paper have been built using Robinson triangles (I, II, Godreche and Orland 1986). For decoration of triangles we

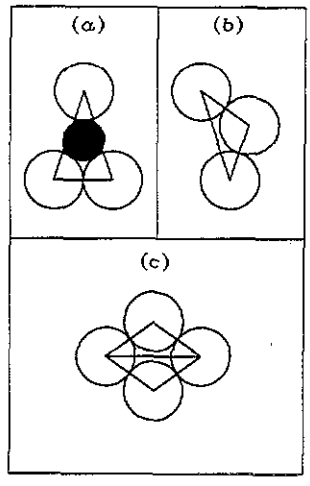

Figure 1. Decoration of the (*a*) big and (*b*) small Robinson triangles with two types of atoms: large ones placed at the corners of each Robinson triangle and small ones at the centres of only big triangles. (*c*) Unstable configuration of large atoms.

used two types of sites (figures 1(*a*) and (*b*)): primary (large) ones in the corners of the triangles and secondary (small) ones in positions inside the big triangles (one per triangle). The bond lengths (Lançon and Billard 1988, Minchau *et al* 1987, Widom *et al* 1987) are equal to

$$d_{LL} = 1 \qquad d_{LS} = d_{LL}/[2\sin(\pi/5)] \qquad d_{SS} = d_{LS}/\tau \tag{1}$$

where L and S denote large and small sites, respectively, and τ is the golden mean value equal to 1.618 . . . . We should note that these two sites do not represent hard discs as $2d_{LS} > d_{LL} + d_{SS}$. All the discussed structures, i.e. Penrose-like structures, twin structures with different concentrations of small Robinson triangles, and random and precipitated structures, decorated in such a way are presented in figures 2(*a*)–(*d*). We have also performed extra analysis for random Penrose tilings, perfect and random crystals and random twins (II). The structure factor was calculated for values of atomic form factors equal to 1 for large sites and 0 for small sites, which gives a direct correspondence to our previous calculations presented in I and II. Modification of the form factor for the small sites changes the diffraction pattern, but it has no influence on the final results of our analysis.

It was shown that a two-component Lennard-Jones system with bond lengths given by (1) in two dimensions spontaneously forms a quasi-crystal (Widom *et al* 1987). In our case most of the structures are near their ground states, as the only source of instability is a local configuration of four large atoms placed in the corners of a rhombus built up by two small triangles (figure 1(*c*)). It can be seen from figure 2 that the Penrose structure and also some twin structures are stable. However, many other structures are unstable, and the number of unstable local configurations increases with deviation from the Penrose tiling concentration. The stability and dynamical properties of our structures will be discussed separately.

3. Five-dimensional representation

As already shown (Jarić 1986, Henley 1988, Tang and Jarić 1990) two-dimensional quasi-crystals obtained by tiling of the plane by thick and thin rhombuses can be

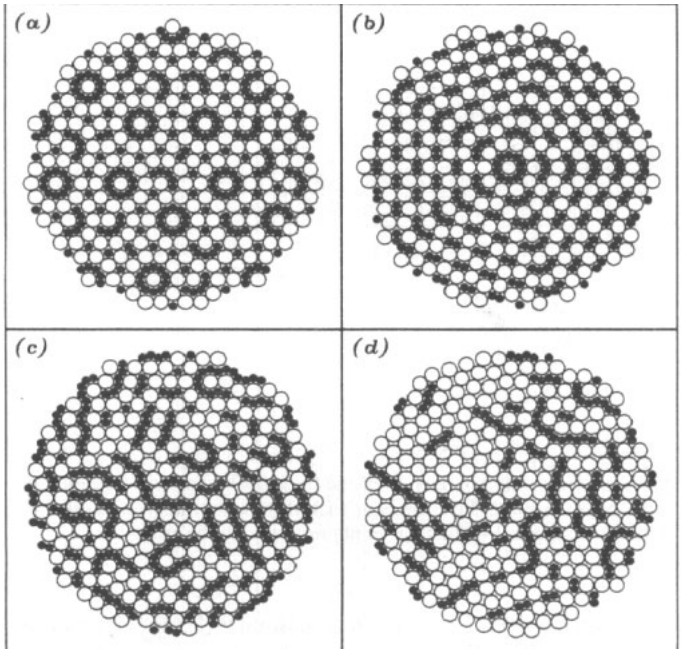

Figure 2. Various types of structure obtained by decoration of Robinson triangles with two types of sites: (*a*) Penrose structure, concentration of small Robinson triangles, $c_P \simeq 0.382$; (*b*) a twin structure ($c = 0.5$); (*c*) a random structure ($c \simeq 0.37$; (*d*) a precipitated structure ($c \simeq 0.77$). Large sites are placed in the corners of the Robinson triangles. Small sites are only centred in the large Robinson triangles.

successfully described by projection of five-dimensional hypercubic lattice sites onto two-dimensional space. The position of any vertex of the tiling is given by five numbers $\{n_\alpha\}$ ($\alpha = 0, \ldots, 4$) such that

$$\boldsymbol{r} = a \sum_{\alpha=0}^{4} n_\alpha \boldsymbol{e}_\alpha \tag{2}$$

where a is a distance between vertices (in our case equal to τ) and

$$\boldsymbol{e}_\alpha = (\cos(2\pi\alpha/5), \sin(2\pi\alpha/5)).$$

Vectors $\boldsymbol{e}_\alpha$ are shown in figure 3.

Perpendicular-space coordinates are given by

$$\boldsymbol{h}(r) = \sum_{\alpha=0}^{4} n_\alpha \boldsymbol{e}_\alpha^{\text{perp}} \tag{3}$$

and

$$h_z(r) = \sum_{\alpha=0}^{4} n_\alpha \tag{4}$$

where

$$\boldsymbol{e}_\alpha^{\text{perp}} = (\cos(4\pi\alpha/5), \sin(4\pi\alpha/5)).$$

Corners of Robinson triangles, which represent the positions of the large sites, can be

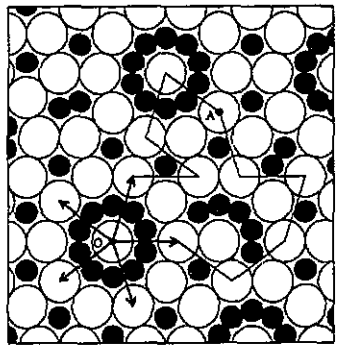

Figure 3. The 5D basis vectors projected onto 2D space are shown around the point O. The position of any big atom can be reached by a sequence of translations given by the basis vectors. As shown for point A, sequences of translations are not necessarily unique. If the sequence is represented by five numbers $(n_0, n_1, n_2, n_3, n_4)$, showing how many times each basis vector has been used, where minus corresponds to a vector in the opposite direction, the representations can differ by (1, 1, 1, 1, 1) or its multiplicity, which is equivalent to a zero translation.

described by five numbers even if the choice of $\{n_\alpha\}$ is not unique (figure 3) as it is for the tiling using thick and thin rhombuses. Parallel- and perpendicular-space components of reciprocal vectors are given by (Tang and Jarić 1990)

$$\boldsymbol{k} = \frac{4\pi}{5a} \sum_{\alpha=0}^{4} m_\alpha \boldsymbol{e}_\alpha \tag{5}$$

$$\boldsymbol{k}^{\text{perp}} = \frac{4\pi}{5} \sum_{\alpha=0}^{4} m_\alpha \boldsymbol{e}_\alpha^{\text{perp}} \tag{6}$$

$$k_z = \frac{2\pi}{5} \sum_{\alpha=0}^{4} m_\alpha. \tag{7}$$

From the dependence of phason-space (perp-space) coordinates on real-space coordinates, the linear terms, called uniform phason strains, can be subtracted by the following operation:

$$\boldsymbol{h}^*(r) = \boldsymbol{h}(r) - a^{-1}\mathbf{E}\boldsymbol{r} \tag{8}$$

$$h_z^*(r) = h_z(r) - a^{-1}\mathbf{E}\boldsymbol{r} \tag{9}$$

where $\mathbf{E}$ is a linear phason strain matrix. Existence of uniform phason strain can be illustrated by the following example. Figures 4(*a*) and (*b*) show maps of phason fields calculated for a crystalline sample with concentration of small Robinson triangles equal to 0.5. The uniform phason strain observed in figure 4(*a*) disappears after transformation given by (8) (see figure 4(*b*)). The same results can be seen from figures 5(*a*) and (*b*), where hodographs of phason fields, calculated before and after reduction of uniform phason strain, are presented. After the linear phason strain subtraction, a continuous distribution of $\boldsymbol{h} = (x_{\text{perp}}, y_{\text{perp}})$ becomes a two-state distribution of $\boldsymbol{h}^*$ shown in figure 5(*b*).

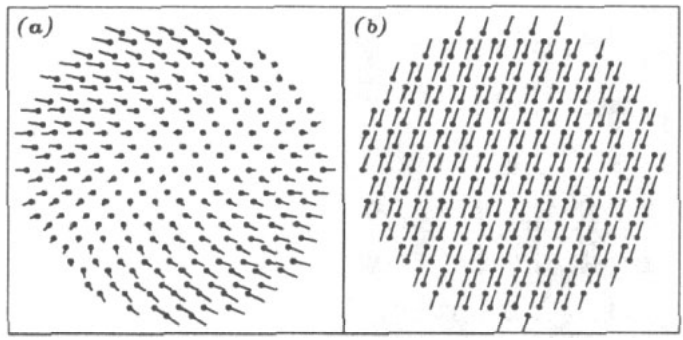

Figure 4. Phason fields, calculated (*a*) before and (*b*) after uniform phason strain subtraction, for a single crystal with equal concentration of small and large atoms. Each arrow placed in parallel space indicates length and direction of perp-space coordinate.

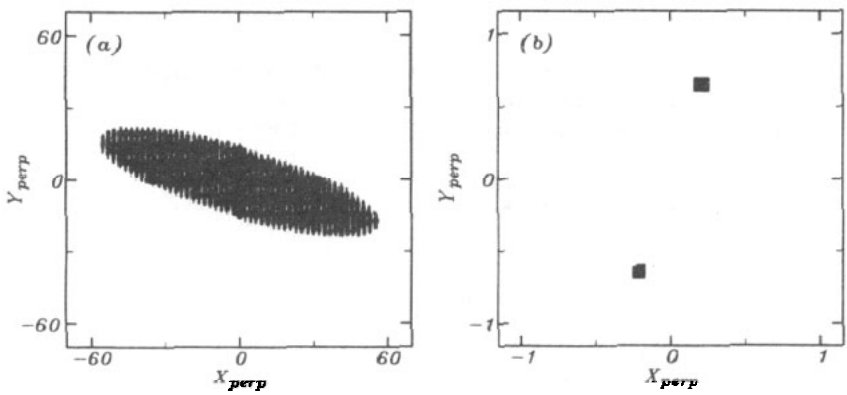

Figure 5. Hodographs of vectors presented in figure 4, (*a*) before and (*b*) after uniform phason strain subtraction.

Figures 6(*a*)–(*d*) and 7(*a*)–(*d*) show phason fields and their hodographs calculated for various structures discussed above. Hodographs from figures 7(*a*)–(*d*) show in fact the window functions used for theoretical calculations of structure factors (Jarić 1986). The phason field for Penrose tiling (figure 6(*a*)) is uniform in real space (i.e. local mean values of $\boldsymbol{h}$ and h^2 are constant over the whole structure) and its distribution (figure 7(*a*)) is bounded and constant in perp-space, which corresponds to constant window function. Phason fields for the twin structures (figure 6(*b*)) are completely different. The local mean value of phason field increases continuously with distance from the centre. The shape of the window function (figure 7(*b*)) corresponds in a way to coherently connected five blocks. Although the structure consists of five individual crystals the global uniform phason strain matrix is equal to zero as it is for Penrose tiling. Phason fields for random

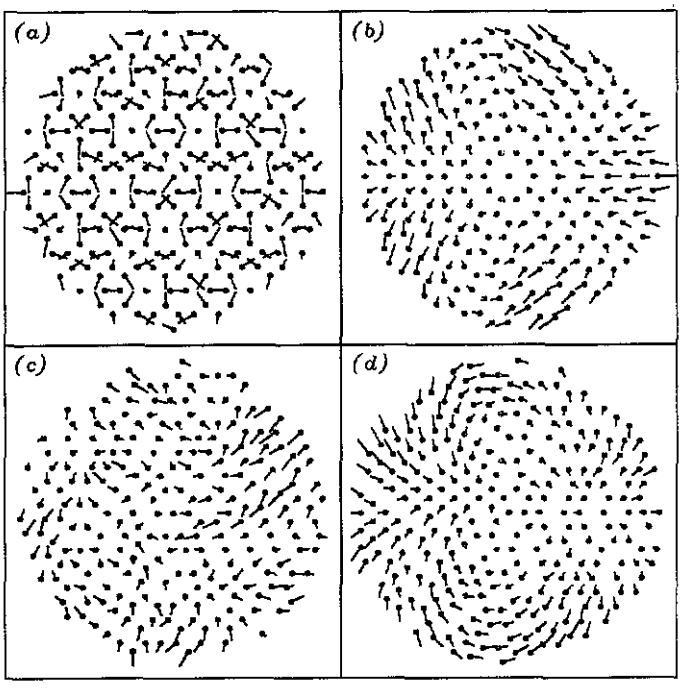

Figure 6. Phason fields of various structures shown in figures 2(*a*)–(*d*): (*a*) for Penrose tiling, (*b*) for twin structure, (*c*) for random and (*d*) for precipitated structures.

and precipitated structures (figures 6(*c*) and (*d*)) look rather complex; however, Gaussian approximation of the window function (figure 7(*c*)) of random structures seems to be reasonable. Uniform phason strains for random and precipitated structures are negligibly small and they have no influence on the results of further calculations. Similar phason fields for grown decagonal packing have been presented by Nori *et al* (1988).

4. Scaling of peak intensities

We performed calculations of peak intensities along the y direction of reciprocal space, and the diffraction patterns have already been presented in I and II. In this direction, for $k_x = 0$, all observed peaks can be divided into groups of peaks, with positions of individual peaks given by

$$k_y = k_0 \tau^n \qquad (n = 0, 1, 2, \ldots). \tag{10}$$

For the first series of peaks $k_0 = 2\pi/[(\tau+2)\sin(\pi/5)] \simeq 2.95$ and indices of peaks are given by

$$\begin{aligned}
&\text{for } n=0 \quad k_y = k_0 \quad \{m_\alpha^0\} = (0,1,0,0,-1) \quad \text{and} \quad k_y^{\text{perp}} = k_0 \\
&\text{for } n=1 \quad k_y = k_0\tau \quad \{m_\alpha^1\} = (0,1,1,-1,-1) \quad \text{and} \quad k_y^{\text{perp}} = -k_0/\tau \\
&\text{for } n \quad k_y = k_0\tau^n \quad \{m_\alpha^n\} = \{m_\alpha^{n-2} + m_\alpha^{n-1}\} \quad \text{and} \quad k_y^{\text{perp}} = k_0(-\tau)^{-n}.
\end{aligned} \tag{11}$$

From (11) it follows that peak indices for the series of peaks given by (10) are described by Fibonacci numbers. Additionally, the sum of indices for a single peak is equal to zero

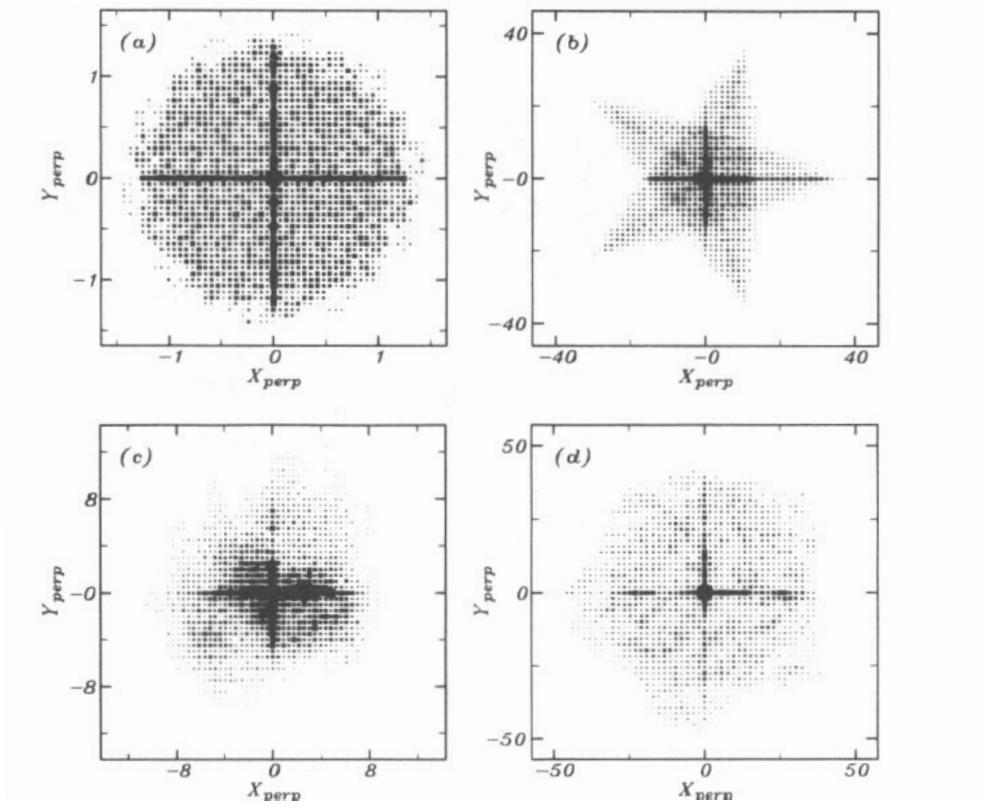

Figure 7. Hodographs of perp-space vectors presented in figure 6: (*a*) for Penrose tiling, (*b*) for twin structure, (*c*) for random and (*d*) for precipitated structures.

($\Sigma m_\alpha = 0$), which, according to (7), gives $h_z = 0$, meaning that the h_z component does not contribute to peak intensities calculated in the y direction.

As mentioned above (see also I and II), the diffraction peak intensities for various twins, and random and precipitated structures do not scale as N^2, contrary to single crystals and Penrose tiling. One of the most important factors influencing the intensities is the Debye–Waller factor. For the phason space this factor depends on the mean-square fluctuation of perpendicular-space coordinate $\boldsymbol{h}$:

$$\langle(\Delta h)^2\rangle = \frac{1}{N}\sum_{j=1}^{N}[\boldsymbol{h}(r_j) - \langle \boldsymbol{h}\rangle]^2. \tag{12}$$

Mean-square values of the phason fluctuations are presented in figures 8(*a*)–(*d*)). For the Penrose tiling, $\langle(\Delta h)^2\rangle$ is independent of the number of sites. For twins, $\langle(\Delta h)^2\rangle$ increases linearly with N and the slope coefficient is concentration-dependent. Also for random and precipitated structures, the linear term is dominant, especially for bigger samples when concentration fluctuations are suppressed. The linear behaviour of $\langle(\Delta h)^2\rangle$ versus N can be explained by simple calculations: twin structures consist of several single

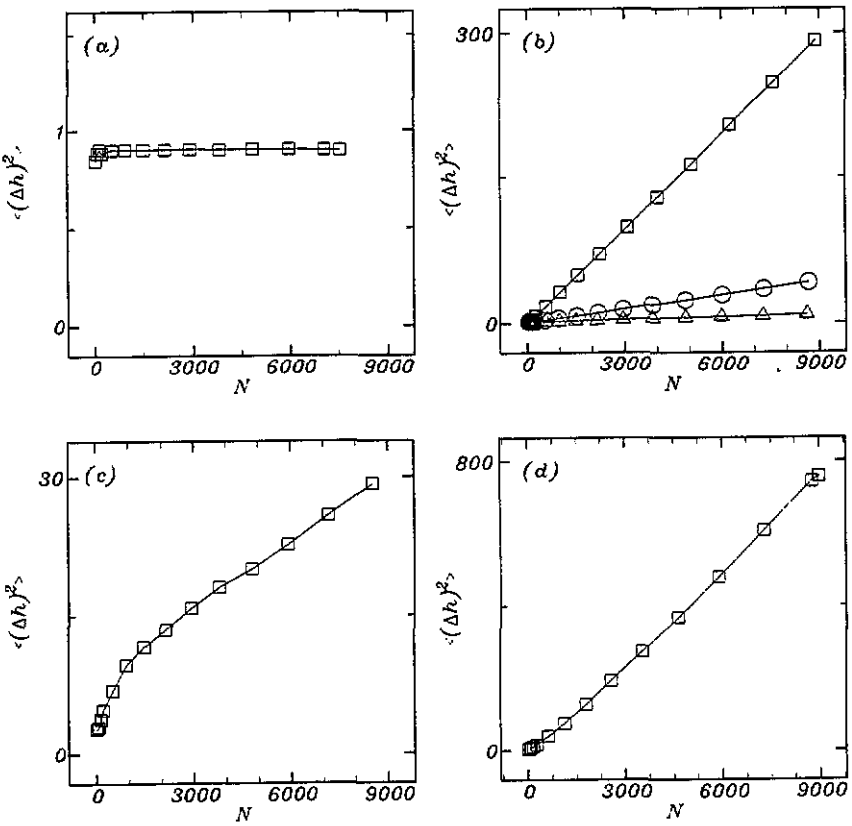

Figure 8. Mean-square value of perp-space fluctuations versus number of large sites for circular samples of: (*a*) Penrose tiling; (*b*) twin structure with $c = 0.5$ (□), $c = 0.4$ (○) and $c = 0.3846$ (△); (*c*) random structure with $c \approx 0.37$; and (*d*) precipitated structure with $c \approx 0.77$. For various twin structures the mean-square value of perp-space fluctuations is linear with the slope coefficient depending on the concentration of small Robinson triangles (see figure 9).

crystals and for each single crystal uniform phason strain determines phason coordinates. It follows that quite generally

$$h(r) \sim \mathbf{E}_0 * r \tag{13}$$

where $\mathbf{E}_0$ is a linear phason strain matrix, which is constant inside a single grain and rotates in a grain boundary. Using a continuous approximation, the mean-square value of Δh is given by

$$\langle(\Delta h^{\text{cont}})^2\rangle = \frac{1}{\pi R^2}\int_0^R |\mathbf{E}_0|^2 r^2 2\pi r \,\mathrm{d}r - \left(\frac{1}{\pi R^2}\int_0^R |\mathbf{E}_0| r 2\pi r \,\mathrm{d}r\right)^2 \tag{14}$$

where $|\mathbf{E}_0|^2 = \lambda_1^2 + \lambda_2^2$ and λ_1, λ_2 are eigenvalues of matrix $\mathbf{E}_0$. This gives

$$\langle(\Delta h^{\text{cont}})^2\rangle = \tfrac{1}{18}|\mathbf{E}_0|^2 R^2.$$

Because $R^2 \sim N$ and $|\mathbf{E}_0| \sim |\mathbf{E}|$ so

$$\langle(\Delta h)^2\rangle \sim |\mathbf{E}|^2 N \tag{15}$$

which means that for twin structures the mean-square value of phason coordinate is

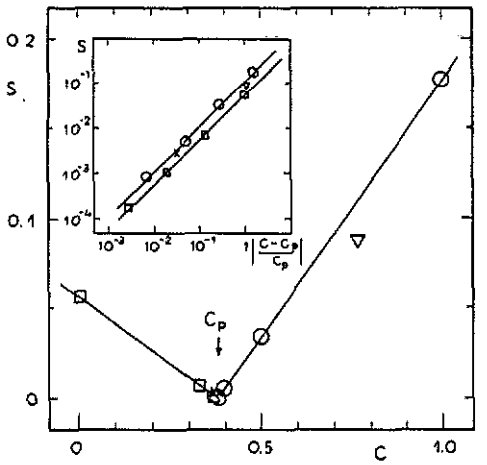

Figure 9. The linear coefficient of mean-square value of perp-space fluctuations on number of sites versus concentration of small Robinson triangles. All the discussed structures (i.e. (□) twins with $c < c_p$, (○) twins with $c > c_p$, (×) random with $c \simeq 0.37$ and (▽) precipitated with $c \simeq 0.77$) indicate a singular point at Penrose concentration $c_p \simeq 382$. Full lines correspond to critical index equal to 1. Inset is the same plot on log–log scale.

proportional to the number of sites and the square of the uniform phason strain for a single grain. This linear dependence on N is in full agreement with our results for twins (figure 8(*b*)) and can also be used for random and precipitated structures (figures 8(*c*) and (*d*)). The slope coefficients obtained for various concentrations are shown in figure 9, indicating a singular point at the Penrose concentration of small Robinson triangles ($c_p = 1/\tau^2 \simeq 0.382$) with critical exponent equal to 1. This value of critical exponent is consistent with (15) and the fact that

$$|\mathbf{E}| \sim N_0^{-1} \sim (\Delta c/c_p)^{1/2} \tag{16}$$

where N_0 is the number of large sites in a unit cell of crystalline structures as shown by the analysis for the rational approximants of Penrose tiling.

The Debye–Waller approximation of peak intensity for phason fluctuations in two dimensions gives

$$I/N^2 = \exp[-0.5(k^{\text{perp}})^2\langle(\Delta h)^2\rangle]. \tag{17}$$

The logarithm of peak intensity normalized to N^2 depends linearly on the mean-square value of perp-space fluctuations, which is fully supported by figures 10(*a*)–(*d*) for all structures discussed. It was found (Elser 1985, Jarić 1986) that, for the series of peaks described by (10), the perp-space coordinate of scattering vectors is given by

$$k_y^{\text{perp}} = k_0^{\text{perp}}(-1/\tau)^n. \tag{18}$$

Knowing formulae (17) and (18) it seems reasonable to rescale the mean-square value of phason fluctuations by a factor of τ^{-2n} to obtain common behaviour for all peaks belonging to the same series of peaks (figures 11(*a*)–(*d*)). The behaviour is generally linear and does not depend on the way the structures have been obtained.

For Penrose tiling with various N, all the peaks belonging to one series (10) give single points lying on a straight line (figure 11(*a*)). For all the other structures (twins,

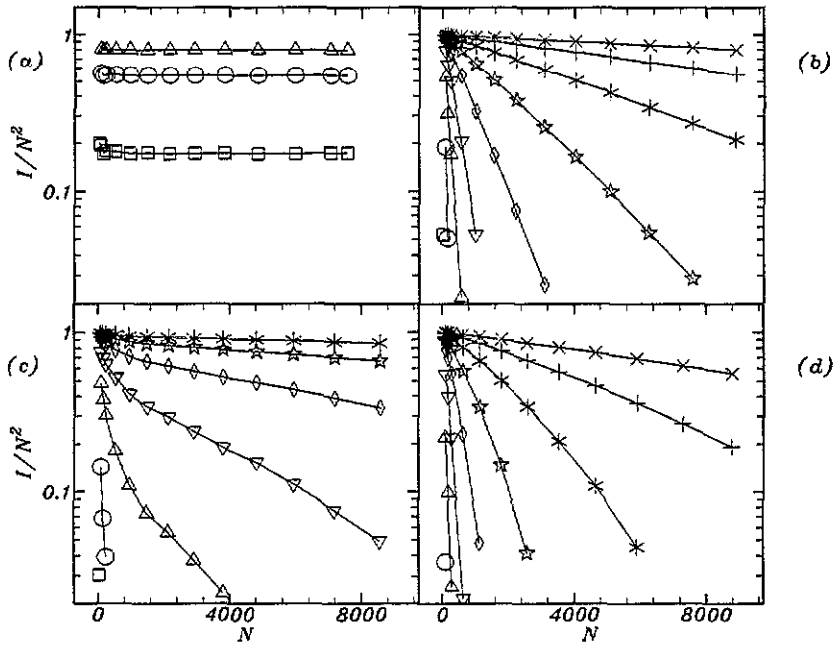

Figure 10. Scaling of peak intensities calculated for a series of peaks given by $k_x = 0$ and $k_y = k_0\tau^n$, where $k_0 = 2.95$, versus number of atoms N: (*a*) for Penrose tiling, (*b*) for twin structure ($c = 0.5$), (*c*) for random ($c = 0.37$) and (*d*) for precipitated ($c = 0.77$) structures. Peak number n indicated as follows: (□) $n = 1$; (○) $n = 2$; (△) $n = 3$; (▽) $n = 4$; (◇) $n = 5$; (☆) $n = 6$; (✳) $n = 7$; (+) $n = 8$; (×) $n = 9$.

random and precipitated) the peak intensities for various N calculated at Penrose positions give points that are placed along the same straight line (figures 11(*b*)–(*d*)). Finally, we can calculate the scaling factor (k/k_P) defined in II. For twins, random and precipitated structures, equations (15), (16) and (17) give

$$\ln(I/N^2) = -C(k^{\text{perp}})^2(\Delta c/c_P)N \tag{19}$$

where C is a constant value. As the scaling factor was defined for equal intensities, from (19) one obtains

$$(k_P^{\text{perp}})^2\langle(\Delta h_P)^2\rangle = 2C(k^{\text{perp}})^2(\Delta c/c_P)N \tag{20}$$

where k_P^{perp} is the perp-space component of the scattering vector, which for the Penrose tiling corresponds to the same intensity as the one found for a given structure, and $\langle(\Delta h_P)^2\rangle$ is a constant value of mean-square phason fluctuations for Penrose tiling. According to (10), (18) and (20) one gets

$$k/k_P \sim (\Delta c/c_P)^{1/2}N^{1/2}. \tag{21}$$

Knowing that $N^{1/2} \sim R$, linear behaviour of scaling factor versus radius of sample is obtained. The similarity parameter A defined as the slope coefficient obtained from plots of k/k_P versus $N^{1/2}$ is proportional to $(\Delta c/c_P)^{1/2}$, which gives a critical exponent equal to 0.5. The higher value of critical exponent (0.55 ± 0.02) obtained in II can be explained by the fact that changing $N^{1/2}$ to R requires corrections for concentration of

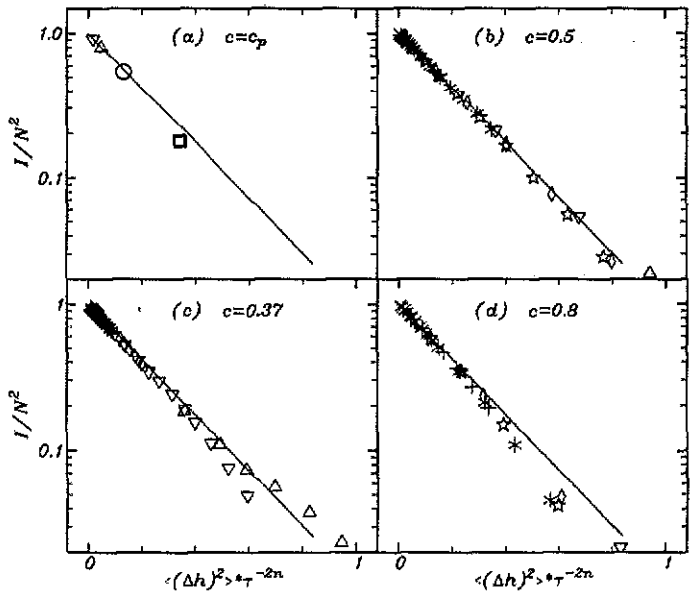

Figure 11. Peak intensities of different structures and different positions of k vector, $k_x = 0$ and $k_y = k_0\tau^n$, with $k_0 = 2.95$ and $n = 1, \ldots, 9$, versus mean value of phason-space fluctuations multiplied by a factor τ^{-2n}: (*a*) for Penrose tiling, (*b*) for twin structure ($c = 0.5$), (*c*) for random ($c = 0.37$) and (*d*) for precipitated ($c = 0.77$) structures. The full line for all figures is the same and represents equation (22) without any free parameter. Peak number n is: (□) $n = 1$; (○) $n = 2$; (△) $n = 3$; (▽) $n = 4$; (◇) $n = 5$; (☆) $n = 6$; (✳) $n = 7$; (+) $n = 8$; (×) $n = 9$.

sites. This concentration of sites (c_S) is a smooth function of c ($c_S = (1 - c)/(2 - c)$) and increases slightly the critical exponent obtained from plots of scaling factor versus R. Additionally, from (17) and (18) it follows that peak intensities for a series of peaks calculated for Penrose tiling are given by

$$I/N^2 = \exp(-\text{const} \times \tau^{-2n}) \tag{22}$$

where const $= (k_0^{\text{perp}})^2\langle(\Delta h_P)^2\rangle/2 \simeq 3.942$, and this equation is an analytical expression for the envelope function defined in II (see also Jarić 1986).

From the above it follows that for concentrations different from c_P the mean-square value of phason fluctuations is proportional to N (15) and the intensity scales according to (19). For the critical concentration this linear term vanishes and the logarithmic term becomes dominant, so the mean-square value of phason fluctuations becomes proportional to $\ln(N)$ (figure 12(*a*)). However, a small deviation of concentration from the critical one, like for random structures with $c \simeq 0.37$, drastically changes this relation and the linear term becomes dominant (see figures 8(*c*) and 12(*b*)). In the case of logarithmic behaviour of $\langle(\Delta h)^2\rangle$ versus N, peak intensities scale as (Tang and Jarić 1990)

$$I/N^2 = N^{-\eta/2} \tag{23}$$

where

$$\eta = \frac{1}{2\pi\kappa}|k^{\text{perp}}|^2 + \frac{1}{2\pi\kappa_z}|k_z|^2 \tag{24}$$

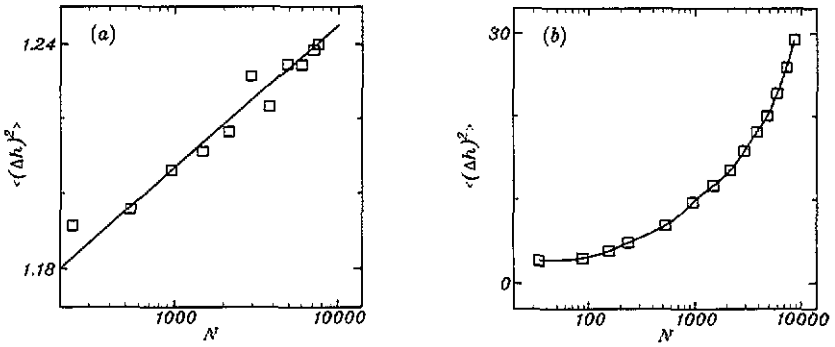

Figure 12. Mean-square value of phason fluctuations versus logarithm of number of large sites. Only for the critical concentration of small Robinson triangles (c_P), i.e. for random Penrose tiling (*a*), is this dependence linear with phason elastic constant equal to 9.6. For all other structures, e.g. for random structure (*b*) (c = 0.37), the logarithmic term is suppressed by the linear term (see figure 8).

κ and κ_z are corresponding phason elastic constants. In our case $k_z = 0$ and the second term in (24) vanishes. The obtained value of phason elastic constant is $\kappa = 9.6$.

5. Conclusions

Various structures obtained by tiling the plane with Robinson triangles can be described by projection from 5D space, although the choice of 5D components is not unique. All the discussed structures, i.e. Penrose tiling, twins, and random and precipitated structures, exhibit quite similar diffraction patterns (I and II). For any finite structure the most intensive peaks are placed at the same positions called Penrose positions. The origin of these peaks and their shapes were already discussed in I and II.

The intensities of peaks calculated at Penrose positions are well approximated by the Debye–Waller factor (17) calculated for phason-space (perp-space) fluctuations. We have calculated such fluctuations and shown that they are constant for Penrose tiling and linear in number of sites for other structures. The slope coefficient of this relation depends linearly on deviation from Penrose concentration, where it exhibits a singular point. For the twin structures, the behaviour mentioned above have been theoretically explained by the existence of uniform phason strains for individual grains of single crystals.

Relation (19) for peak intensities gives linear behaviour of the scaling factor from II on radius of the sample. Additionally, the similarity parameter defined in II scales with deviations from Penrose concentration, with critical exponent equal to 0.5, if scaling is discussed as a function $N^{1/2}$. In our previous paper (II) this scaling factor was calculated as a function of R, which slightly increased the critical exponent to 0.55 ± 0.02 because of a concentration-dependent correction for $N(R)$ dependence.

The slope coefficient of the linear relation of $\langle(\Delta h)^2\rangle$ versus N vanishes for the critical concentration and the logarithmic term starts to dominate, changing the scaling of the peak intensities to that given by (23) and (24) with phason elastic constant $\kappa = 9.6$. Finally, we have checked the validity of the Debye–Waller approximation for phason fluctuations of all discussed structures. For the series of peaks given by (10) we have

shown that after scaling of mean-square fluctuations by a factor τ^{-2n} (where $n = 0, 1, 2, \ldots$ is the peak number in the series) all the logarithms of peak intensities are well approximated by theoretically derived straight line with slope coefficient equal to $-0.5(k_0^{perp})^2$.

For Penrose tiling the peak intensities normalized to N^2 and mean-square fluctuations of phason coordinates are constant, while peak intensities of other structures as well as their phason fluctuations depend on number of sites. The results are universal for all the structures, and the points are placed along a single straight line, common to all the discussed structures.

Acknowledgments

We would like to thank M V Jarić for encouragement and helpful suggestions. This work was partially supported by the Polish Ministry of Education Research Project.

References

De Bruijn N G 1981 *Proc. Konink. Ned. Acad. Wetensch.* A **84** 39
Elser V 1985 *Phys. Rev.* B **32** 4892
—— 1986 *Acta Crystallogr.* A **42** 36
Field R D and Fraser H L 1984 *Mater. Sci. Eng.* **68** L17
Godreche C and Luck J M 1989 *J. Stat. Phys.* **55** 1
Godreche C and Orland H 1986 *J. Physique Coll.* **47** C3 197
Henley C L 1988 *J. Phys. A: Math. Gen.* **21** 1649
Jarić M V 1986 *Phys. Rev.* B **34** 4685
Kramer P 1985 *Z. Naturf.* **40** 775
Kramer P and Neri R 1984 *Acta Crystallogr.* A **40** 580
Lançon F and Billard L 1988 *J. Physique* **49** 249
Lebech B, Wolny J and Pytlik L 1988 *Quasicrystalline Materials* ed C Janot and J M Dubois (Singapore: World Scientific) p 234
Minchau B, Szeto K Y and Villain J 1987 *Phys. Rev. Lett.* **58** 1960
Nori F, Ronchetti M and Elser V 1988 *Phys. Rev. Lett.* **61** 2774
Onoda G Y, Steinhardt P J, DiVincenzo D P and Socolar J E S 1988 *Phys. Rev. Lett.* **60** 2653
Pauling L 1985 *Nature* **317** 512
—— 1987 *Phys. Rev. Lett.* **58** 365
Penrose R 1974 *Bull. Inst. Math. Appl.* **10** 266
—— 1979 *Math. Intell.* **2** 32
Shechtman D, Blech I, Gratias D and Cahn J W 1984 *Phys. Rev. Lett.* **53** 1951
Stephens P W and Goldman A 1986 *Phys. Rev. Lett.* **56** 1168
Strandburg K J, Tang L-H and Jarić M V 1989 *Phys. Rev. Lett.* **63** 314
Tang L-H and Jarić M V 1990 *Phys. Rev.* B **41** 4524
Widom M, Deng D P and Henley C L 1989 *Phys. Rev. Lett.* **53** 30
Widom M, Strandburg K J and Swedsen R H 1987 *Phys. Rev. Lett.* **58** 706
Wolny J, Pytlik L and Lebech B 1988 *J. Phys. C: Solid State Phys.* **21** 2267
—— 1990 *J. Phys.: Condens. Matter* **2** 785